Identification of leaching-controlling process by differential acid neutralization analysis for geochemical modeling

– application to metal hydroxide sludge stabilization with coal fly ash –

Olivier Peyronnard[a] ; Denise Blanc[a] ; Mostafa Benzaazoua[b] ; Pierre Moszkowicz[a]

[a] LGCIE Site Carnot, INSA-Lyon, 9, rue de la Physique, F69621, France
[b] UQAT, 445 Blvd de l'Université, Rouyn –Noranda, Québec, Canada J9X 5E4

Abstract

The modeling of the leaching behavior of cementitious materials containing wastes requires the identification of the minerals reacting in contact with aqueous media. The differential analysis of acid neutralization data permits to highlight the dissolutions of phases occurring during the acidification of the solid matrix. Nevertheless, the identification of these dissolving phases is fairly complex because of the influences of the geochemical context on the cementitious hydrates stability. In this work, we propose to use a numerical simulator as an aid tool for the identification of the dissolving hydrated minerals. This work is based on the results of a differential acid neutralization analysis test performed on synthetic hydroxide sludge stabilized/solidified by hydraulic binders. The proposed method permits the identification of semi-validated mineral assemblages representing the studied materials and their leaching behavior.

Introduction

During their storage, wastes stabilized/solidified by hydraulic binders can react with aqueous media. That induces a certain weathering of the solid matrix and a possible release of the pollutants that contains. To make sure of the absence of risk for the environment, wastes storage scenarios should be environmentally assessed. These assessment studies require a determination of the leaching behavior of the stabilized/solidified wastes. This is classically studied through different leaching tests: acid neutralization capacity, influence of pH on elements release, leachable fraction… Tests results are, then, extrapolated to the real scenarios to predict the pollutants mobilization and the potential risks for environment. Extrapolations, generally, result of a numerical simulation of the waste behavior in the envisaged scenario. Geochemical models were shown to be able to predict the leaching from cementitious materials [1]. Being based on the equilibrium laws between solid and liquid phases, these models require a minimal knowledge of the mineral composition of the studied material. The mineralogy of cementitious matrix can be approached by various techniques. X-ray diffractometry (XRD), and thermal analysis inform on the nature of the main mineral phases. Electronic microscopy (SEM-EDS) can be used to localize elements; in particular pollutants. Nevertheless, XRD only permits the identification of well crystallized phases whereas cementitious matrixes are mainly composed of amorphous minerals. Furthermore, the size of hydrated cement phases is in order of SEM resolution, so localization of elements remains imprecise.

Glass and Buenfeld [2] propose a mathematical treatment of acid titration curves permitting a numerical interpretation of the leaching behavior of cementitious matrixes. This treatment

consists in plotting the quantity of acid needed to involve an evolution of pH of 1 unity (dH^+/dpH) against the pH. This "differential acid neutralization analysis" transforms the titration curve to a spectrum of discrete peaks. Each peak results of the dissolution of a particular mineral present in the matrix. Thus, this differential analysis should permit the identification of the hydrated cement phases governing the leaching behavior. Moreover, the area embraced by each peak represents to the acid consumption needed for the dissolution of the related phase [2]. Therefore, this method permits a semi-quantification of the cementitious phases present in the matrix.

However, hydrated cement phases stability is influenced by leachate composition and interactions (interferences and/or precipitation phenomenon) with other mineral phases [3, 4]. So identification of the phase responsible for each peak is fairly complex without a minimum knowledge of the material mineralogy [2]. Leachate chemistry can provide a substantial help [5, 6, 7]. For each peak, the release of the main elements (Ca, Si, Al, Fe, SO_4^{2-}) informs on the nature of the dissolving mineral. Pollutants mobilization informs on their hosts and retention mechanisms. Because leachate composition evolves upon minerals dissolution, analysis can be limited to the solutions surrounding each peak [7].

This work deals with the links between the mineralogy and the leaching behavior of stabilized/solidified sludge doped with chromium and zinc. These links were studied by coupling "classical" mineralogical analyses (XRD and SEM-EDS) and a differential acid neutralization analysis. This combination of two different approaches should lead to a better understanding of the leaching behavior: dissolutions of principal cementitious hydrates and their repercussions on the release of pollutants. Then, a model (mineral assemblage) able to represent the behavior of the main hydrates because they are controlling the evolution of the pH and, thus, the release of pollutants is proposed. Numerical simulation were performed using USGS's software PHREEQC [8], that has been successfully used to model the leaching behavior of cement stabilized/solidified wastes [1, 9-10]. This study was performed on the case of synthetic hydroxide sludge stabilized/solidified by hydraulic binders composed of ordinary Porltand cement and coal fly ashes.

Materials and methods

Materials

Hydroxide sludge containing iron, zinc and hexavalent chromium were synthesized at the laboratory. To do this, acidic solution containing zinc, iron and hexavalent chromium were neutralized by sodium hydroxide. Two different binders were used: pure Ordinary Portland Cement (OPC) and a mix of 50 % of OPC and 50 % of class F Fly Ashes (PFA). PFA (Surschiste's Silicoline®) come from the combustion of pulverized coal in an electric power station. After a 28 days curing in obscurity, hydration reactions were stopped by immersion in acetone and drying at 40°C [11]. A part of the obtained mortars were cut in $4*4*4$ cm^3 blocks for additional test. The remaining parts were crushed to a particle size inferior of 1 mm and stocked in obscurity and dried conditions.

Four distinct materials were analyzed (Table 1): two blanks (OPC and OPC-PFA) corresponding to binders and two stabilized sludge by pure cement (OPC-S) or fly ashes added to cement (OPC-PFA-S).

Table 1: Formulations of the four studied materials

Ref.	OPC	PFA	Dried Sludge	Water
OPC	100 g	0	0 g	40 mL
OPC-PFA	50 g	50 g	0 g	40 mL
OPC-S	86.8 g	0	13,2 g	46 mL
OPC-PFA-S	43,4 g	43,4 g	13,2 g	48 mL

Method

Differential acid neutralization analysis

Acid neutralization data were obtained by adding predetermined quantities of acid (0 to 3.8 mol/L) to about 12.5 g of powdered material at a liquid/solid ratio equal to 4. A series of 20 batch tests were undertaken to obtain a pH evolution from natural pH (pH of equilibrium of the solid with pure water) to a pH between 9 and 10. Batch tests were performed in a rotary shaker during a period of 8 days to get total equilibrium between the liquid and solid phases. Leachates were, then, filtered to 0.45 μm on a Büchner filter and conductivity and pH were measured. The solutions after each peak (Figure 2) were analyzed by ICP AES for Ca, Al, Si, Fe, Cr, Zn, Mg, K and Na (norm NF EN ISO 11885). Sulfate and chloride were analyzed by ionic chromatography (norm NF EN ISO 10304-2). Concentrations are given with an uncertainty of 10%.

The differential analysis used in this work slightly differs from those proposed by Glass and Buenfeld [2]. Derivative (dH^+/dpH) is calculated using a centered difference scheme; explicit and implicit schemes were used for the extrema. To smooth spectra, a linearly interpolated point was added between each two experimental points. In their works, Glass *et al.* [2, 5, 6] calculate the derivative using an explicit scheme. Spectra are, then, plotted considering no variation of the derivative between each two points. Smoothed spectra can then be obtained using a moving average. We also add to Glass's protocol the measurement of conductivity. Indeed, the evolutions of conductivity could be interpreted in terms of conductivity evolution induced by a unit pH change (dC/dpH). The same mathematical treatment was used to plot the conductivity spectra.

$$\left(\frac{dH^+}{dpH}\right)_i = \frac{H^+_{i+1} - H^+_{i-1}}{pH_{i+1} - pH_{i-1}}$$

$$\left(\frac{dH^+}{dpH}\right)_1 = \frac{H^+_2 - H^+_1}{pH_2 - pH_1}$$

$$\left(\frac{dH^+}{dpH}\right)_N = \frac{H^+_N - H^+_{N-1}}{pH_N - pH_{N-1}}$$

with i index of the batch, and N total number of batch.

Modeling

Methodological framework for the identification of minerals

The identification of reactive minerals within cementitious composites using a numerical simulator is based on the assumption that numerical simulation permits to calculate the pH of dissolution of various hydrated phases in various environments. Thus, the comparison between simulated and experimental results should help for the identification of the cementitious hydrates. This comparison also inform on the reaction path and the possible precipitations occurring during the acid attack.

A five steps framework was followed to identify the mineral assemblages (mix of pure phases and solid solutions) representing the tested materials:

1. Estimation of the mineral phases potentially present or which could precipitate based on:

− The knowledge of the studied material (bibliographic study, previous works…);

− A mineralogical study by direct methods: XRD, SEM-EDS. Other methods like FTIR or thermal analysis can also be used;

− The identification of phases potentially at equilibrium with the analyzed leachates by calculations of saturation index [12].

2. Simulation of the acid attack on simplified mineral assemblages issued from the previous step. These simulations permit the compilation of a bank of spectra adapted to the studied case. For cementitious materials like cement stabilized wastes, it is interesting to simulate the behaviors of cementitious composite considering the presence of portlandite and/or CSH.

3. Minerals identification and quantification:

− Identification of the cementitious hydrates by comparison of the simulated and experimental spectra.

− Quantification from the area embraced by peaks and from the leachable fraction or the total content of elements.

4. Simulation of the behavior of the mineral assemblage determined at the previous step and comparison with experimental results. This comparison is made on the differential analysis spectra, the titration curves and the release of elements. Step 3 and 4 are reiterated until the obtaining of an acceptable simulation.

5. Validation of the identified mineral assemblage by comparison of the simulated and experimental results of a leaching test conducted under different conditions. In our case, the validation was made on a pH dependence test realized at a liquid/solid ratio of 10.

In this paper, the results presented are partial. For example, the phases 1 and 5 will not be presented. The complete study can be read in Peyronnard *et al*. [13 - 14].

Hypotheses of simulation

Acid attacks were simulated using the USGS's software PHREEQC [8]. PHREEQC is a geochemical calculations software based on the laws of equilibrium between solid, liquid and gas phases. The following hypotheses were considered for the simulations:

− The equilibrium between liquid and solid is reached, no gas phase is considered.

− Cementitious phases are considered as pure phases (EQUILIBRIUM_PHASES) or as forming ideal solid solutions (SOLID_SOLUTIONS). No sorption mechanisms are considered. Phases, which could precipitate during the leaching, are integrated in the mineral assemblage with an initial amount equal to 0.

− Amorphous CSH are integrated in the thermodynamic database considering 3 CSH having a Ca/Si ratio equal to 1.8, 1.1 and 0.8 to model their non congruent dissolution [9]. In the mineral assemblage, they are considered as forming a solid solution in order to smooth the transition from the CSH rich in calcium to the CSH poor in calcium.

As in most of geochemical calculations softwares, thermodynamic data are, in PHREEQC regrouped in a thermodynamic database. To be pertinent, the proposed methodology needs a database as exhaustive as possible. So, a database dedicated to hydrated cement materials containing zinc and chromium was compiled. The equilibrium constants for the dissolution reactions of the identified minerals are presented in Table 2. The database compilation shows divergences on solubility products between authors, even for well known phases like portlandite. We, generally, choose to use the more quoted in the literature values (log K_1).

The thermodynamic database was compiled to be the most exhaustive as possible. Nevertheless the solubility products of some phase like unhydrated cement (C_2S, C_3S, C_3A and C_4AF) have not been found in the literature. Such phases can't have been introduced in the database. The Table 1 presents only the dissolution reactions and their solubility products of the minerals identified as present in the studied materials or as precipitating during the acid attack. The tests being conducted on a limited range of pH (between 9 and 13), the phases, like calcite ($CaCO_3$), dissolving out of the studied range were not considered.

Table 2: Reactions and equilibrium constants for minerals considered in the minerals assemblages representing the four studied materials

Mineral	Reaction	Log K_1 [ref]
Portlandite	$Ca(OH)_2 + 2H^+ \leftrightarrow Ca^{2+} + 2H_2O$	22.8 [8]
Brucite	$Mg(OH)_2 + 2H^+ \leftrightarrow Mg^{2+} + 2H_2O$	16.84 [8]
$Zn(OH)_2$	$Zn(OH)_2 + 2H^+ \leftrightarrow Zn^{2+} + 2H_2O$	11.9 [15]
Ca-hydroxyzincate	$CaZn_2(OH)_6 : 2H_2O + 6H^+ \leftrightarrow Ca^{2+} + 2Zn^{2+} + 8H_2O$	43.9 [16]
Gypsum	$CaSO_4 : 2H_2O \leftrightarrow Ca^{2+} + SO_4^{2-} + 2H_2O$	-4.581 [19]
$Al(OH)_3$(am)	$Al(OH)_3 + OH^- \leftrightarrow Al(OH)_4^-$	0.24 [17]
$Fe(OH)_3$(am)	$Fe(OH)_3 + 3H^+ \leftrightarrow Fe^{3+} + 3H_2O$	5 [8]
SiO_2(am)	$SiO_2 + 2H_2O \leftrightarrow Si(OH)_4$	-2.714 [15, 16, 19]

C_2ASH_8	$Ca_2Al_2O_5SiO_2 : 8H_2O \leftrightarrow 2Ca^{2+} + 2Al(OH)_4^- + SiO(OH)_3^- + OH^- + 2H_2O$	-20.49 [18]

CSH		
CSH1.8	$(CaO)_{1.8}SiO_2 : 1.8H_2O + 3.6H^+ \leftrightarrow 1.8Ca^{2+} + Si(OH)_4 + 1.6H_2O$	32.6 [9]
	$Ca_{1.8}SiO_{3.8} : H_2O + 3.6H^+ \leftrightarrow 1.8Ca^{2+} + Si(OH)_4 + 0.8H_2O$	
CSH1.1	$(CaO)_{1.1}SiO_2 : 1.1H_2O + 2.2H^+ \leftrightarrow 1.1Ca^{2+} + Si(OH)_4 + 0.2H_2O$	16.7 [9]
	$Ca_{1.1}SiO_{3.1} : H_2O + 2.2H^+ \leftrightarrow 1.1Ca^{2+} + Si(OH)_4 + 0.1H_2O$	
CSH0.8	$(CaO)_{0.8}SiO_2 : 0.8H_2O + 1.6H^+ + 0.4H_2O \leftrightarrow 0.8Ca^{2+} + Si(OH)_4$	11.1 [9]
	$Ca_{0.8}SiO_{2.8} : H_2O + 1.6H^+ + 0.2H_2O \leftrightarrow 0.8Ca^{2+} + Si(OH)_4$	

AFm		
Al-Monosulfate	$(CaO)_3Al_2O_3CaSO_4 : 12H_2O \leftrightarrow 4Ca^{2+} + 2Al(OH)_4^- + SO_4^{2-} + 4OH^- + 6H_2O$	-29.43 [20]
Fe-Monosulfate	$(CaO)_3Fe_2O_3CaSO_4 : 12H_2O \leftrightarrow 4Ca^{2+} + 2Fe(OH)_4^- + SO_4^{2-} + 4OH^- + 6H_2O$	-32.02 [18]
Cr-Monophase	$(CaO)_3Al_2O_3CaCrO_4 : 15H_2O \leftrightarrow 4Ca^{2+} + 2Al(OH)_4^- + CrO_4^{2-} + 4OH^- + 9H_2O$	-30.38 [21]
Al-Monocarbonate	$(CaO)_3Al_2O_3CaCO_3 : 11H_2O \leftrightarrow 4Ca^{2+} + 2Al(OH)_4^- + CO_3^{2-} + 4OH^- + 5H_2O$	-31.47 [18]
Fe-Monocarbonate	$(CaO)_3Fe_2O_3CaCO_3 : 11H_2O \leftrightarrow 4Ca^{2+} + 2Fe(OH)_4^- + CO_3^{2-} + 4OH^- + 5H_2O$	-35.79 [18]
Friedel's Salt	$(CaO)_3Al_2O_3CaCl_2 : 10H2O \leftrightarrow 4Ca^{2+} + 2Al(OH)_4^- + 2Cl^- + 4OH^- + 4H_2O$	-28.8 [10]
C_4AH_{13}	$(CaO)_4Al_2O_3 : 13H_2O \leftrightarrow 4Ca^{2+} + 2Al(OH)_4^- + 6OH^- + 6H_2O$	-27.49 [22]
	$(CaO)_4Al_2O_3 : 13H_2O + 14H^+ \leftrightarrow 4Ca^{2+} + 2Al^{3+} + 20H_2O$	
C_4FH_{13}	$(CaO)_4Fe_2O_3 : 13H_2O \leftrightarrow 4Ca^{2+} + 2Fe(OH)_4^- + 6OH^- + 6H_2O$	-29.88 [15]

AFt		
Ettringite	$Ca_6Al_2(SO_4)_3(OH)_{12} : 26H_2O \leftrightarrow 6Ca^{2+} + 2Al(OH)_4^- + 3SO_4^{2-} + 4OH^- + 26H_2O$	-45.09 [18]
	$Ca_6Al_2(SO_4)_3(OH)_{12} : 26H_2O + 12H^+ \leftrightarrow 6Ca^{2+} + 2Al^{3+} + 3SO_4^{2-} + 38H_2O$	
Fe-Ettringite	$Ca_6Fe_2(SO_4)_3(OH)_{12} : 26H_2O \leftrightarrow 6Ca^{2+} + 2Fe(OH)_4^- + 3SO_4^{2-} + 4OH^- + 26H_2O$	-49.49 [18]
Cr-Ettringite	$Ca_6Al_2(CrO_4)_3(OH)_{12} : 26H_2O \leftrightarrow 6Ca^{2+} + 2Al(OH)_4^- + 3CrO_4^{2-} + 4OH^- + 26H_2O$	-41.46 [21]
Al-tricarbonate	$Ca_6Al_2(CO_3)_3(OH)_{12} : 26H_2O \leftrightarrow 6Ca^{2+} + 2Al(OH)_4^- + 3CO_3^{2-} + 4OH^- + 26H_2O$	-41.3 [18]

Results and discussion

Differential acid neutralization analyses

Titration curves (Figure 1) show typical results with:

- a titration curve of pure cement (OPC) showing three major plateaus which is in accordance with data from literature [2, 3];

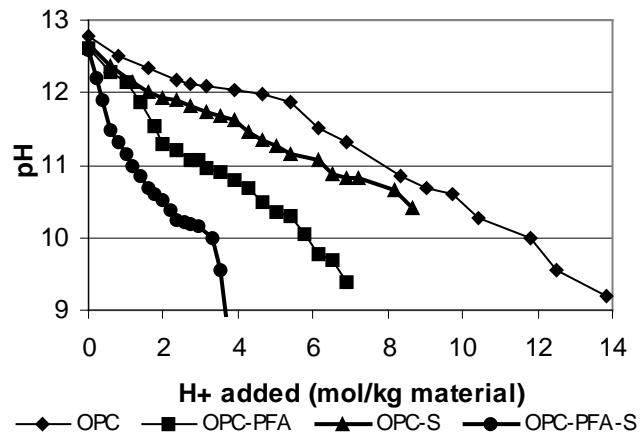- a loss of neutralization capacity for materials incorporating fly ashes or sludge [3].

Figure 1. Titration curves of the four studied materials.

The loss of resistance to acidification is explained by modifications of hydration reactions and products, in particular a decrease of the portlandite amount. This decrease can be explained by the dilution of OPC in the binder. For OPC-PFA and OPC-PFA-S, the pouzzolanic reactions consume portlandite and PFA to form CSH [23]. This decrease of portlandite amount induces a loss of acid neutralization capacity explaining the absence of plateau for pH around 12. The gap between OPC-S and OPC curves could be due to an inhibition of hydration caused by the presence of zinc in the sludge [11, 24-25].

For each solidified material, the differential analysis of acid added (dH^+/dpH) and of conductivity evolutions (dC/dpH) give two spectra having the same shape (Figure 2). This likeness is due to the influence of acid addition on conductivity. Furthermore, dissolution and precipitation also induce evolutions of the conductivity because of variations of the ionic content. Therefore, small differences appear between the two spectra, in particular in the amplitude of peaks. Nevertheless, the conductivity spectrum permit to confirm the presence of small peaks appearing on the acid added spectrum. So, these "twin" peaks are complementary and their plotting exhibits the dissolution of each hydrated cement phase resisting to the acidification.

OPC spectrum consists of five peaks at pH around 12.4, 12.1, 11.4, 10.6 and 10.1. For pH under 10, an increase of dH^+/dpH is noticed, but, the lack of data prevents the confirmation of the existence of this peak. Therefore, as suggested by Glass and Buenfeld [2], the leaching behavior of OPC is controlled by the dissolution of five hydrates, among portlandite, ettringite and CSH.

For the three other materials, spectra consist in more than five peaks, some of them are very close. The leaching behavior of OPC-S seems to be controlled by six mineral phases dissolving respectively at pH around 12.2, 11.9, 11.7, 11.4, 11.1 and 10.8. Others hydrates probably dissolve at pH under 10, but, because of the lack of experimental data, their occurrence can't be confirmed. Figure 2 shows seven dissolutions during the acidification of OPC-PFA (pH around 12.2, 11.3, 11.1, 10.9, 10.7, 10.3 and 9.7) and OPC-PFA-S (pH around 12, 11.4, 11.1, 10.9, 10.6, and a double peak around 10.2).
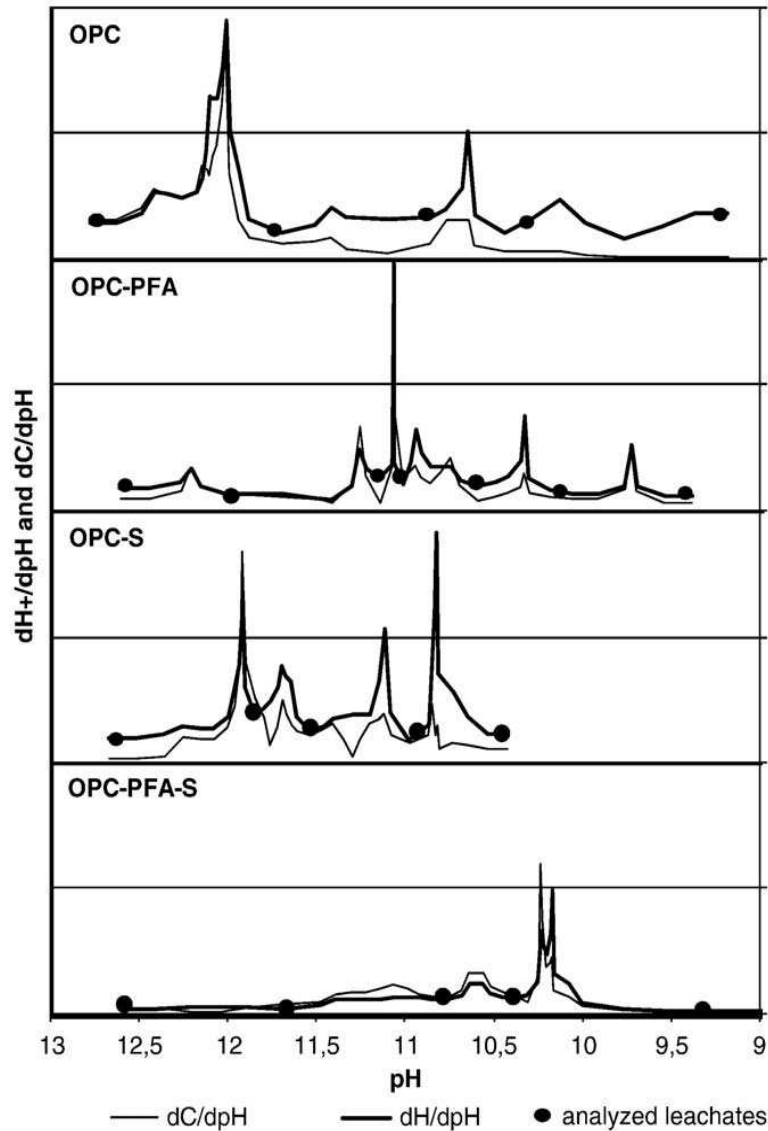

Figure 2. Differential analyses spectra of the four studied materials.

The comparison of the differential analysis spectra of the four studied materials (Figure 2) reveals three main differences:

- Decrease/Increase in peak intensity;

- Gaps of pH of minerals dissolution: for example, the first peaks for OPC and OPC-S are gapped of 0.1 unit of pH, whereas they probably result of the dissolution of the same mineral;

- Apparition of new peaks, for example, the peak occurring at pH around 11.7 for OPC-S.
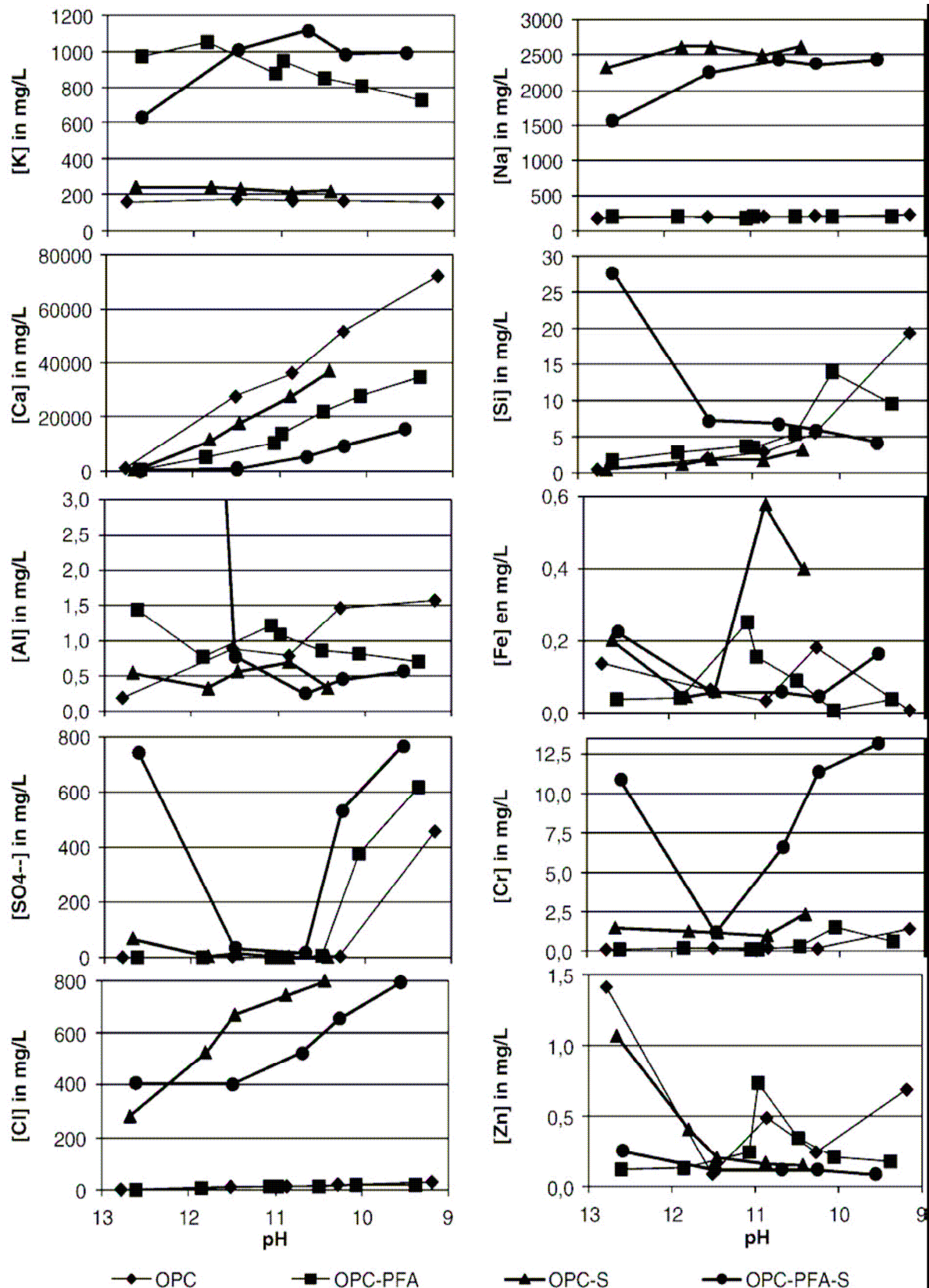
Figure 3. Evolutions of the release of elements against the pH for the four materials.

Variations of peaks intensity reflect the variations of the amount of the related hydrated phase. Thus the peak appearing at pH around 12.1, probably due to portlandite dissolution [2], is weaker for the materials containing ashes (OPC-PFA and OPC-PFA-S). This decrease is

explained by portlandite consumption by pouzzolanic reactions and the decrease of OPC amount in the binder.

The stability of cementitious hydrates depends of the composition of the leachate and so, of the presence of other minerals in the solid. As example, if portlandite is present in the initial solid matrix, its dissolution liberates calcium, delaying the dissolution of the other minerals containing calcium. The elements leached can, also, favor the dissolution of hydrated phases in profit of the precipitation of a new phase. For example, the presence of sulfate in the leachate could favor the dissolution of aluminates because of ettringite precipitation. Therefore, the pH of dissolution of a hydrated phase depends of the geochemical context.

The peaks observed only for particular materials probably results of the dissolution of a phase initially present in sludge or ashes or of a hydration product resulting of the interactions between the binder and sludge.

Release of elements

Some leachates of each material were analyzed (Figure 2). Figure 3 presents the release of each element among the pH. Except for K and Na, elements are released dependently of the pH. Some elements, like Al or Fe, remain weakly soluble on the studied range of pH, whereas others (Ca, Si, SO_4^{2-}) are highly leached (Figure 3).

For the four materials, calcium concentration increases all along the decrease of pH due to Ca presence in most cementitious hydrates. Nevertheless, the observed decrease of portlandite amount (peak occurring for pH around 12.1) is reflected in Ca mobilization in the first times of the acid attack.

Silicon had a similar behavior for OPC, OPC-PFA and OPC-S with a slight increase of release from natural pH (pH obtain at the equilibrium between the matrix and pure water) to a pH around 10 - 10.5 where a significant increase is observed. Silicon being principally contained into CSH, peaks appearing below pH 10 could be identified as resulting of the dissolution of CSH. However, CSH dissolution is non congruent [26] and probably occurs gradually all along the decrease of pH. The decalcification of CSH, being progressive, probably doesn't result in peaks on the differential analysis spectra. Nevertheless, their "final" dissolution (dissolution of the siliceous structure) probably leads to the occurrence of a peak. For OPC-PFA-S, the silicon leaching curve shows a greater release at natural pH (12.6) than for lower pH. This could be due to the remaining of non hydrated cement or to the precipitation of silicon in a phase highly soluble in basic conditions.

For the four materials, the sulfate is released for pH under 10.2. The leaching of sulfate is therefore, probably controlled by the same mineral in the 4 materials: Ettringite or Al-monosulfate and/or their ferric analogs. For the two materials containing sludge (OPC-S and OPC-PFA-S), a decrease of the sulfate release can be observed in the first time of the acid attack (pH between 12.6 and 11.8). This behavior can be explained by:

 – the occurrence of sulfate under a soluble form (gypsum for example) and its reprecipitation (ettringite for example) with the elements (Al, Fe) liberated by the dissolution of other hydrates;

 – the occurrence of sulfate under a form having a solubility increasing in highly basic conditions (pH > 11.8).

With an increase for pH under 10.2, the release of chromium appears as linked to sulfate one. That can be explained by a substitution of sulfate by chromate in AFt or AFm phases. Indeed, sulfates can be, in these phases, substituted by heavy metals oxyanions (CrO_4^{2-}, AsO_4^{2-}…). These cementitious hydrates play an important role in heavy metal retention [11]. For OPC-PFA-S, the leaching of chromium decreases between natural pH and pH around 11.5. Like for sulfate, this behavior could be due to occurrence of chromium under a soluble form in the unleached material and its precipitation with the calcium and aluminum released or to the occurrence of chromium as a phase whose solubility is increasing in highly basic conditions.

The release of aluminum remains globally relatively low on the studied range of pH. For OPC, the leaching of aluminum increases a first time for pH between 12.8 and 11.5 and a second time for pH between 10.9 and 10.3. The two relative peaks are probably caused by the dissolution of aluminate phases. For OPC-PFA and OPC-S, aluminum is mainly leached for pH between 11.8 and 10.3. So, the peaks appearing in this range of pH can be attributed to the dissolution of aluminate phases. For OPC-PFA-S, aluminum is more released under basic conditions, maybe due to a lack of binder hydration.

As aluminum one, iron concentrations in leachates remain weak. However, its variation permit to establish hypothesis on the origin of peaks observed on differential analysis spectra. For OPC, the leaching of iron increases between pH 10.7 and 10.2, the related peak is, then, probably caused by the dissolution of a ferrite analog of the aluminate phase previously mentioned. For OPC-PFA and OPC-S, the dissolution of a ferrite mineral appears for the peak around pH 11.3 - 11.4. No peak seems to be linked to iron dissolution in the case of OPC-PFA-S.

The behavior of zinc seems to be dependent of the nature of the binder and of the presence of sludge. Indeed when pure cement is used as binder (OPC and OPC-S), the release of zinc decreases for pH between 12.7 and 11.5, whereas it remains weak for binders containing fly ashes (OPC-PFA and OPC-PFA-S). Furthermore, the leaching of zinc is maximal for pH around 11 for the two materials without sludge (OPC and OPC-PFA) whereas it remains weak for OPC-S and OPC-PFA-S. This behavior could be induced by the dissolution of a zinc hydrated phase immediately followed by zinc reprecipitation under a less soluble form. This hydrated phase could be calcium hydroxyzincate [27-28].

Magnesium has a similar behavior for the four materials with an increase of leaching from pH around 10. The release of magnesium seems to be independent of peaks apparition. Chloride can't be, here, considered as a soluble (element released independently of the pH) in particular for OPC-PFA-S and OPC-S. For natural pH, the release of chloride is relatively low but increases right from the start of acid attack. Chloride could appear as Friedel's or Kuzel's salt (respectively $(CaO)_3.Al_2O_3.CaCl_2:10H_2O$ and $(CaO)_3.Al_2O_3.CaCl(SO_4)_{0.5}:10H_2O$) and their ferrite analogs [6] which dissolution have been reported for pH around 12 [29].

Simulation results

The table 3 presents the mineral assemblages used to represent the behavior of the four studied pastes when submitted to an acid neutralization test. For each paste, phases are set, in the mineral assemblage, at their identified amount in the solid. Phases, set at an amount equal to 0, are not present in the unleached material, but precipitate during the leaching process.

Table 3: Mineral assemblages representing the four studied materials

Phases	OPC	OPC-PFA	OPC-S	OPC-PFA-S
Portlandite	0.55 (EP)	0.20 (EP)	0.1 (EP)	0.02 (EP)
Brucite	0.02 (EP)	0.035 (EP)	0.015 (EP)	0.03 (EP)
$Zn(OH)_2$	8.10^{-5} (EP)	0 (EP)	0 (EP)	0 (EP)
Ca-Hydroxyzincate		1.10^{-5} (EP)	7.5e-3 (EP)	$7.5.10^{-3}$ (EP)
C_2ASH_8	0 (EP)	0 (EP)	0 (EP)	0.045 (EP)
CSH1.8	0.5 (SS)	0.05 (SS)	0.2 (SS)	0.06 (SS)
CSH1.1	0.25 (SS)	0.5 (SS)	0.2 (SS)	0.3 (SS)
CSH0.8	0 (SS)	0 (SS)	0 (SS)	0 (SS)
Al-monosulfate	0.03 (SS)	0.04 (SS)		
Fe-monosulfate	0.01 (SS)	0.04 (SS)	0.07 (SS)	0.025 (SS)
Cr-Monophase	9.10^{-5} (SS)	3.10^{-5} (SS)	0 (SS)	0 (SS)
Al-Monocarbonate	0.18 (SS)	0.06 (SS)	0.08 (SS)	0.01 (SS)
Fe-Monocarbonate	0.08 (SS)	0.03 (EP-DO)	0.1 (EP-DO)	0.02 (EP)
Friedel's Salt			0.015 (SS)	
Ettringite	0.04 (SS)	0.01 (SS)	0.01 (SS)	0.005 (SS)
Fe-Ettringite	0.02 (SS)			
Cr-Ettringite	0 (SS)	0 (SS)	2.10^{-5} (SS)	0 (SS)
Al-Tricarbonate	0 (SS)	0.01 (SS)	0.01 (SS)	0.04 (SS)
C_4AH_{13}			0.06 (SS)	
C_4FH_{13}			0.06 (SS)	

SS: Solid Solution; EP: Equilibrium Phases; DO: Dissolve Only. Phases' amounts are expressed in mol/L of leachate.

The four materials are composed of the same main hydrates: portlandite, CSH, AFm and AFt phases. The influence of fly ashes and sludge on cement hydration reactions consists principally in variations of the amount of phases. As example, the consumption of portlandite by pouzzolanic reactions in presence of fly ashes is clearly demonstrated for OPC-PFA and OPC-PFA-S. For OPC-S and OPC-PFA-S, a relative augmentation of the amounts of AFm and AFt phases is observed. This phenomenon can be attributed to an inhibition of C_2S and C_3S hydration inducing a relative augmentation of amounts of the hydration products of C_3A and C_2AF. For these two materials, sulfates appear principally as ettringite whereas for OPC and OPC-PFA, they occur as monosulfate. This difference can be explained by sludge sulfates content (4.4 % in mass). Indeed, hydration of C_3A products ettringite that is progressively transformed in aluminum monosulfate with the decrease of sulfates concentration. For materials containing sludge, sulfates content being higher, this transformation is probably limited. The absence of a phase in an assemblage may not mean its absence in the represented material. However, its influence on the leaching behavior can be neglected.
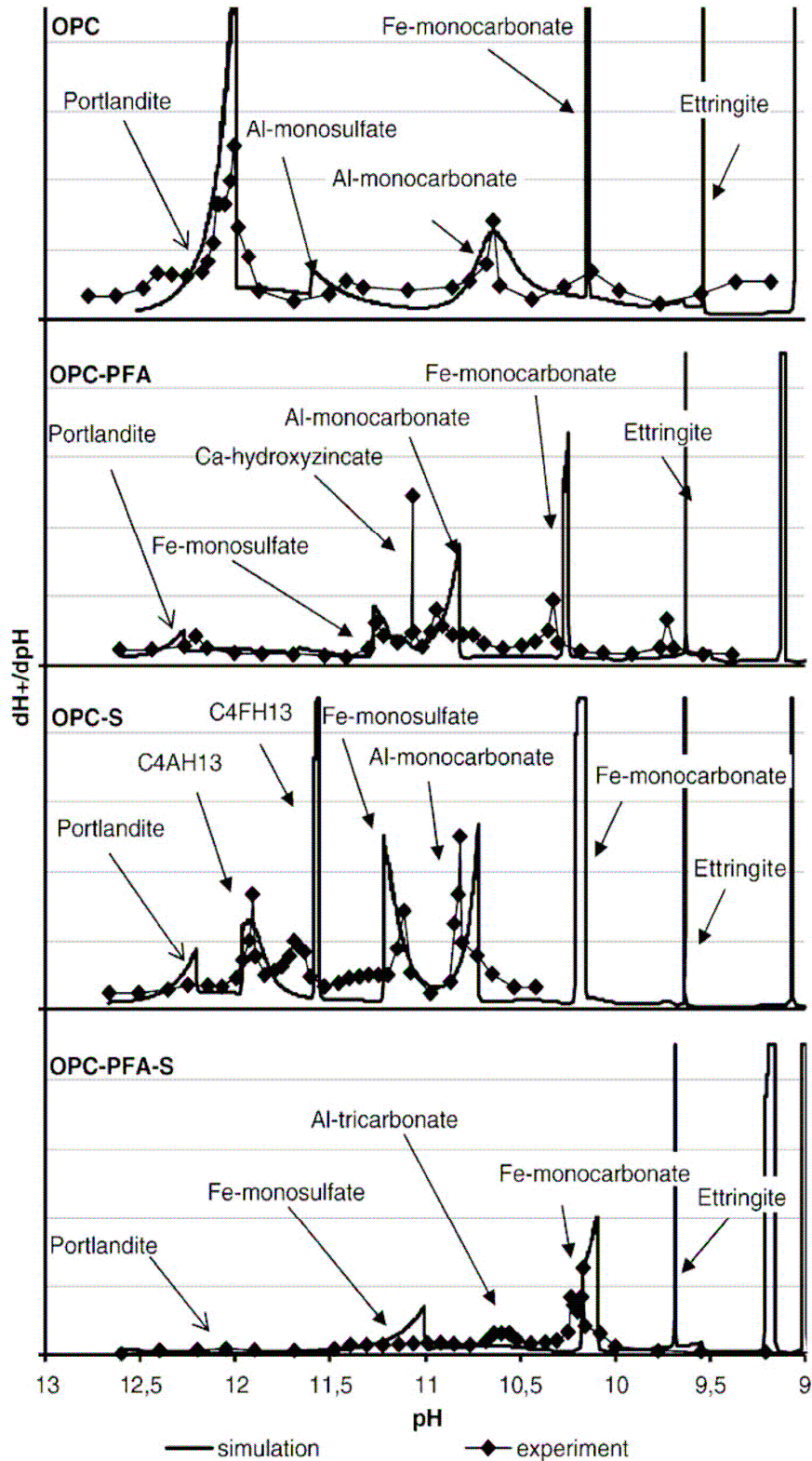
Figure 4 Identification of the mineral assemblages : experimental and simulated spectra.

The Figure 4 represents the experimental and simulated spectra. It can be seen in this figure that the pH evolution of leachate is, mainly, controlled by the dissolution of three groups of hydrates :

- The peak observed around pH 12 - 12.2 is caused by the dissolution of portlandite (Figure 1). The quantification (Table 2) show a reduction of portlandite formed for materials

containing sludge or ashes. For OPC-S, a peak of high intensity appears for a pH of 11.9. This peak could be identified as corresponding to the dissolution of portlandite. Nevertheless no reason was found to explain the "delay" of its dissolution. The dissolution of C_4AH_{13} could, also, be at the origin of this peak. This hypothesis is backed up by the attribution to the dissolution of C_4FH_{13} of the peak appearing at pH equal 11.7.

- Peaks, observed between pH 11.5 and 10, are essentially caused by the dissolution of AFm phases. High pH peaks (up to 11) result of the dissolution of aluminum and iron monosulfate. For pH under 11, the observed peaks result of the dissolution of aluminum and iron monocarbonate. AFm phases, being known as forming solid solutions [30,31], are generally considered as such. This hypothesis permits to smooth curves and link the behaviors of the different components of a solid solution. It also permits a better representation of chromium release.

- Peaks appearing for pH below 10 are caused by the dissolution of AFt phases, C_2ASH_8 and CSH. However, our results did not permit to clearly highlight their occurrence because of a lack of data for pH under 10. Sulfate and silicon behaviors give some important informations. For example, sulfate leaching can't be properly represented without the introduction of ettringite in the mineral assemblages. Besides, the release of silicon reveals the dissolution of CSH. Like for AFm phases, AFt are considered as forming solid solutions.

The identification of the minerals reacting during the acidification is made by comparison of simulated and experimental spectra and by comparing the leaching of elements (Figure 5). Indeed a mineral assemblage can give a correct differential analysis spectrum but being unable to simulate correctly the release of elements. Because of the difference of leaching behavior induced by variations of the mineral amounts, the hydrates quantification has to be made simultaneously of their identification. For example, Fe-monocarbonate appears in both OPC-PFA and OPC-PFA-S, but its dissolution is observed at pH around 10.3 for OPC-PFA and around 10.2 for OPC-PFA-S. This gap is due to aluminum tricarbonate dissolution: present in larger quantity in OPC-PFA-S, its dissolution delays Fe-monosulfate ones. Hydrated cement phases are, in a first time, quantify from the acid consumption of their dissolution (area embraced by peaks) and are refined by fitting simulation results on titration curves and/or elements release.

Figure 5 presents, as example, the curves of release of elements for OPC-PFA-S. The leaching of the different elements is relatively well represented. For calcium, the simulated release is a little to high for pH under 11. A better representation could be obtained by reducing the AFm phase amount, but then, the acid neutralization capacity became too weak. The proportion of CSH1.8 and CSH1.1 also play an important role in the release of calcium and in the shape of the titration curve. For the four materials, the simulated release of silicon becomes too high for pH under 10. This can be explained by a too high solubility of amorphous silica (SiO_2). Aluminum and iron are present in various cementitious hydrates (AFm, AFt…) and possibly reprecipitate under new forms (AFt, amorphous hydroxides). This induces variations of release that are hardly represented with a simplified mineral assemblage. Nevertheless, the identified mineral assemblages permit to simulate correctly the most important evolutions of leaching. The control by ettringite dissolution of the release of sulfate is clearly demonstrated for the four materials. For OPC and OPC-PFA, ettringite is too soluble in highly basic conditions to represent correctly the observed mobilization but considering sulfate as AFm gives good results. In highly basic conditions, the release of sulfates is controlled by monosulfate. Then, ettringite precipitates from the sulfate and aluminum liberated and

controls the leaching. The association of chromium and sulfates leaching is modeled by a substitution of sulfate by chromate in AFm and AFt phases which are modeled as solid solutions. The release of zinc is modeled considering zinc hydroxide and calcium hydroxyzincate. Nevertheless, these two phases are too soluble in the more basic conditions. Magnesium is globally well represented by brucite, in spite of a too high solubility for pH under 10.5.
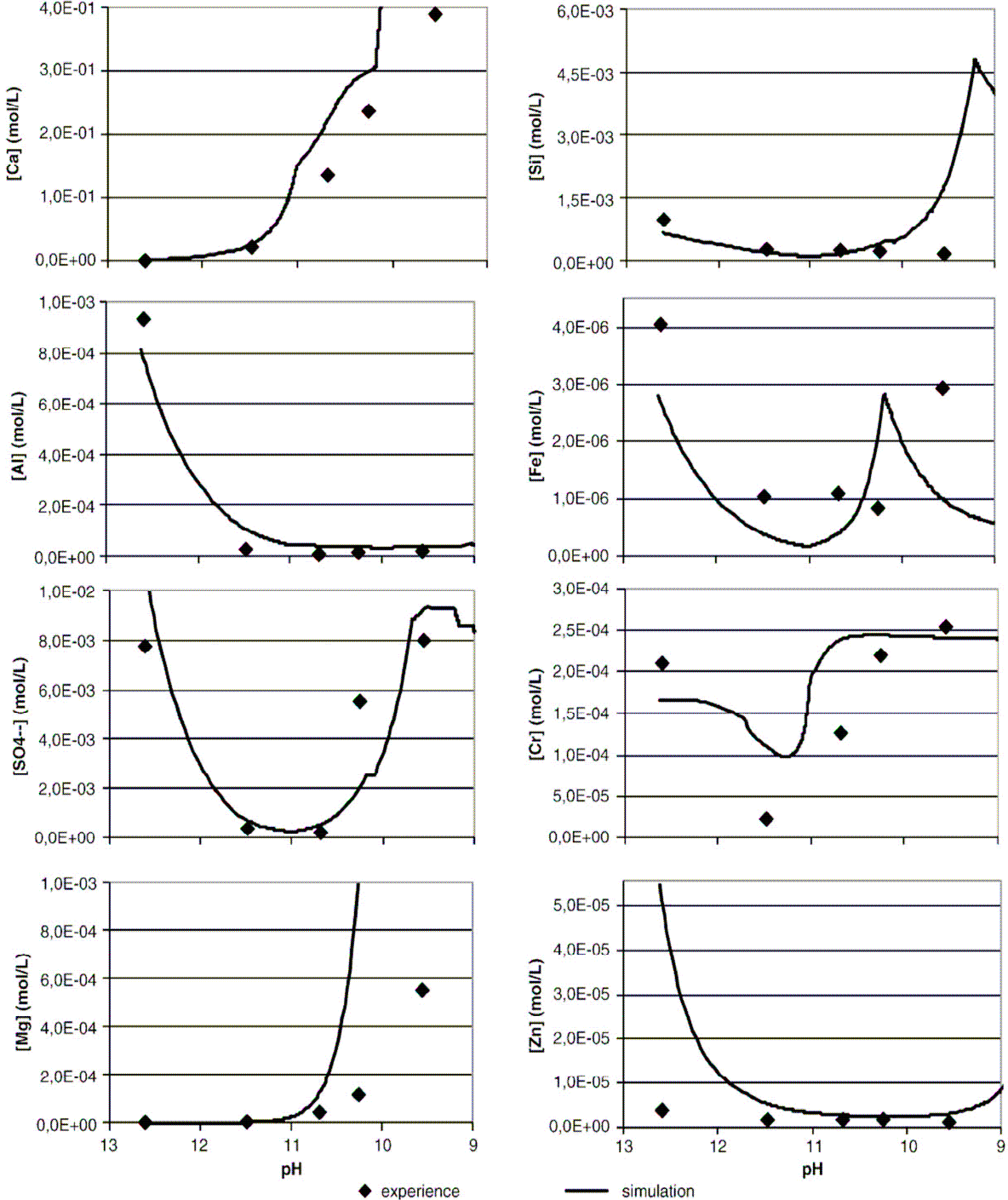

Figure 5. Experimental and simulated leaching curves of OPC-PFA-S.

Conclusion

This study deal with the identification of the cementitious hydrates governing the leaching behavior of synthetic hydroxide sludge stabilized/solidified by a hydraulic binder. In this work, the possibility of using a numerical simulator as an aid tool to interpret acid neutralization results is proposed and tested. The identification of the reactive minerals was based not only on saturation index calculations but also on the study of hydrated cement phases stability in various geochemical contexts.

Differential acid neutralization analysis is a useful tool to help in characterizing mineral materials like concrete or cement stabilized/solidified wastes.

References

[1] C.E. Halim, S.A. Short, J.A. Scott, R. Amal, G Low, Modelling the leaching of Pb, Cd, As, and Cr from cementitious waste using PHREEQC, Journal of Hazardous Materials A215 (2005) 45-61.
[2] G.K. Glass, N.R. Buenfeld, Differential acid neutralisation analysis, Cement and Concrete Research 29 (1999) 1681-1684.

[3] J.A. Stegemann, R.J. Caldwell, C. Shi, Response of various solidification systems to acid addition, in: J.J.J. Goumans, G.J. Senden, H.A. van der Sloot (Eds.), Waste Materials in Construction: Putting Theory into Practice, Studies in Environmental Science 71, Elsevier Science, Amsterdam, 1997, pp 803-814.

[4] J.A. Stegemann, C. Shi, Waste acid resistance of different monolithic binders and solidified wastes, in: J.J.J. Goumans, G.J. Senden, H.A. van der Sloot (Eds.), Waste Materials in Construction: Putting Theory into Practice, Studies in Environmental Science 71, Elsevier Science, Amsterdam, 1997, pp 551-562.

[5] G.K. Glass, B. Reddy, N.R. Buenfeld, Corrosion inhibition in concrete arising from its acid neutralization capacity, Corrosion Science 42 (2000) 1587-1598.

[6] G.K. Glass, B. Reddy, N.R. Buenfeld, The participation of bound chloride in passive film breakdown on steel in concrete, Corrosion Science 42 (2000) 2013-2021.

[7] E. Fried, M. Benzaazoua, B. Bussière, T. Belem, Study of the leaching behaviour and metal fixation within cemented paste backfill materials. 9th International Symposium in Mining with Backfill. Organized by the Canadian Institute of Mining, Metallurgy and Petroleum (CIM). Montreal, Quebec, Canada, April 29-May 2, 2007.

[8] D.L. Parkhurst, C.A.J. Appelo, User's guide to Phreeqc (version 2) – a computer program for speciation, batch-reaction, one-dimensional transport, and inverse geochemical calculations, Water-Resources Investigations Report 99-4259, Denver, Colorado 1999.

[9] L. De Windt, R. Badreddine, modeling of long-term dynamic leaching tests applied to solidified/stabilsed waste, Waste Management 27 (2007) 1638-1647.

[10] J.V.jr Bothe, P.W. Brown, PhreeqC modelling of Friedel's salt equilibria at 23°C, Cement and Concrete Research 34 (2004) 1057-1063.

[11] J.N. Diet, Stabilisation/Solidification des déchets : Perturbation de l'hydratation du ciment Portland par les substances contenues dans les boues d'hydroxydes métalliques. Ph D Thesis, INSA de Lyon, 1996.

[12] H.A. van der Sloot, A. van Zomeren, J.J. Dijkstra, J.CL. Meussen, R.N.J. Comans, H. Scharf, Prediction of the leaching behaviour of waste mixture by chemical speciation modelling based on a limited set of key parameters, ECN RX 05-164, 2005.

[13] O. Peyronnard, M. Benzaazoua, D. Blanc, P. Moszkowicz Study of mineralogy and leaching behavior of stabilized/solidified sludge using differential acid neutralization analysis. Part 1 Experimental study, Cement and Concrete Research (2009)

[14] O. Peyronnard, D. Blanc, M. Benzaazoua, P. Moszkowicz Study of mineralogy and leaching behavior of stabilized/solidified sludge using differential acid neutralization analysis. Part 2. Use of numerical simulation as an aid tool for cementitious hydrates identification, Cement and Concrete Research (2009),

[15] LLNL database supplied with Phreeqc

[16] F. Ziegler, C.A. Johnson, The solubility of calcium zincate ($CaZn_2(OH)_6.2H_2O$), Cement and Concrete Research 31 (2001) 1327-1332.

[17] A. Capmas, D. Ménétrier-Sorrentino, The effect of temperature on the hydration of calcium aluminate cement. UITECR'89 (1989) pp 1157-1170, cited by [14]

[18] B. Lothenbach, F. Winnefeld, Thermodynamic modelling of the hydration of Portland cement, Cement and Concrete Research 36 (2006) 209-226.

[19] W. Hummel, U. Berner, E. Curti, F.J. Person, T. Thoenen, Nagra/PSI Chemical Thermodynamic Data Base 01/01, Universal Publishers, 2002.

[20] D. Damidot, F.P. Glasser, Thermodynamic investigation of the $CaO-Al_2O_3-CaSO_4-H_2O$ system at 50 and 85°C, Cement and Concrete Research 22 (1992) 1179-1191.

[21] R.G. Perkins, C.D. Palmer, Solubility of chromate hydrocalumite ($3CaO.Al_2O_3.CaCrO_4,xH_2O$), Cement and Concrete Research 31 (2001) 1741-1748

[22] E.J. Reardon, An ion interaction model for the determination of chemical equilibria in cement/water systems, Cement and Concrete Research 20 (1990) 175-192.

[23] F.P. Glasser, Fundamental aspects of cement solidification and stabilization, Journal of Hazardous Materials 52 (1997) 151-170.

[24] J.D.Ortego, Y. Barroeta, F.K. Cartledge, H. Akhter, Leaching effects on silicate polymerization. An FTIR and Si-NMR study of lead and zinc in Portland cement, Environmental Science and Technology 25 (1991) 1171-1174.

[25] D. Stephen, R. Mallman, D. Knöfel, R. Härdtl, High intakes of Cr, Ni and Zn in clinker. Part II : Influence on the hydration properties, Cement and Concrete Research 29 (1999) 1959-1967.

[26] R. Duval, H. Hornain, La durabilité du béton vis à vis des eaux agressives, In: J. Baron, J.P. Ollivier, La durabilité des bétons. Presses de l'Ecole Nationale des Ponts et Chaussées (1992) pp 351-389.

[27] G. Arliguie, J.P. Ollivier, J. Grandet, Etude de l'effet du zinc sur l'hydratation de la pâte de ciment Portland, Cement and Concrete Research 12 (1982) 79-86.

[28] A. Stumm, K. Garbev, G. Beuchle, L. Black, P. Stemmermann, R. Nüesch, Incorporation of zinc into calcium silicate hydrates, part I: formation C-S-H with C/S=2/3 and its isochemical counterpart gyrolite, Cement and Concrete Research 35 (2005) 1665-1675.

[29] U.A. Birnin-Yauri, F.P. Glasser, Friedel's salt, $Ca_2Al(OH)_6(Cl,OH) 2H_2O$: its solid solutions and their role in chloride bonding, Cement and Concrete Research 28 (12) (1998) 1713-1723.

[30] F.P. Glasser, A., Kindness, S.A. Stronach, Stability and solubility relationships in AFm phases. Part I: chloride,sulphate and hydroxide, Cement and Concrete Research 29 (1999) 861-866

[31] T. Matschei, B. Lothenbach, F.P. Glasser, The AFm phase in Portland cement. Cement and Concrete Research 37 (2007) 118-130.